# Subchannelization Performance for the Downlink of a Multi-Cell OFDMA System

Carle Lengoumbi, Philippe Godlewski, Philippe Martins
Telecom-Paris, Ecole Nationale Supérieure des Télécommunications
LTCI-UMR 5141 CNRS
46 rue Barrault 75013 Paris, France
Email: {carle.lengoumbi, philippe.godlewski, philippe.martins}@enst.fr

***Abstract*—In this paper, different subchannelization modes for the downlink of a multi-cell OFDMA system are investigated. The frequency reuse factor is one. The subchannelization mode FUSC adopted in 802.16 is considered: frequency collision problem and partial loading are addressed. For a full loading factor, performances are compared with dynamic subcarrier allocation algorithms.**

*Index Terms*— **IEEE 802.16, multi-cell, OFDMA, partial loading, subchannelization.**

## I. Introduction

The Orthogonal Frequency Division Multiple Access (OFDMA) is a promising multiple access technique which combines Orthogonal Frequency Division Multiplexing (OFDM) modulation scheme and the Frequency Division Multiple Access technique (FDMA). It benefits of two main advantages of OFDM: inter symbol interference (ISI) mitigation and high data rates support. OFDMA has been chosen for IEEE 802.16-2004 ([1]) and its extension for mobility support IEEE 802.16e ([2]). OFDMA divides the bandwidth into several subsets which are allocated to distinct users. A multi-user diversity gain can be achieved since a subcarrier in deep fade for a user may be good for another. However, different users may have the same best subcarriers. Subcarrier assignment is a tough problem.

Some contributions consider that subcarriers are assigned individually ([3]-[6]) which requires a per subcarrier channel state information (CSI) knowledge. In [3], the total transmit power is minimized accounting for user rate requirements. This problem is denoted as Margin Adaptive optimization (MA). The "dual" problem called Rate Adaptive optimization (RA) concerns cell rate maximization subject to a power constraint ([4]-[6]). The authors of [4], show that in one cell, a subcarrier should be assigned to one user at a time to maximize the cell rate. In [5]-[6], the authors consider minimum user rate constraints in the RA problem. The basic Dynamic Assignment algorithm (bDA, [5]) and the Rate Profit Optimization algorithm (RPO, [6]) are proposed for subcarrier assignment. The bDA algorithm is interesting for its simplicity. The RPO algorithm handles situations where users have the same best subcarrier (referred to as conflicts) in an efficient manner. In presence of user rate constraints ([3], [5]-[6]), subcarrier assignment is commonly preceded by the determination of the number of subcarriers for each user.

In [1]-[2], a constant number of subcarriers are grouped before being allocated. Two ways to form subchannels are respectively called diversity and contiguous subchannelization. Diversity subchannelization (e.g. FUSC, Fully Used SubChannels) draws subcarriers pseudo-randomly to form a subchannel. Regarding contiguous subchannelization, subcarriers of a subchannel are adjacent.

In this paper, we are interested in comparing FUSC with contiguous subchannelization and dynamic subcarrier allocation algorithms proposed in RA ([5]-[6]). In RPO and bDA, each user receives a fixed number of subcarriers to allow comparisons with FUSC. The remainder of the paper is organized as follows. Section II describes the channel model and the system parameters. Section III presents the pseudo-random subchannel composition of IEEE 802.16 and the problem of frequency collisions in a multi-cell context. Dynamic subcarrier allocation (DSA) is investigated in section IV. In section V, practical modulation and coding schemes (MCS) are used to evaluate spectral efficiency. The frequency reuse factor is set to one and partial loading of FUSC subchannels is considered. Section VI concludes the paper.

## II. System model

### A. Channel modeling

The channel model consists of $N$ parallel narrowband subcarriers over the bandwidth $W$. The path loss model is $K\, d(u)^{-\alpha}$ where $d(u)$ is the distance between a given user $u$ and his serving base station (BS), $\alpha$ is the pathloss exponent ($2 \leq \alpha \leq 4$) and $K$ is a constant for a given environment. The shadowing effect is modelled using a lognormal distribution variable $a_{sh}$ ($10\log(a_{sh})$ is $\mathcal{N}(0, \sigma^2_{sh})$ with $4\text{ dB} \leq \sigma_{sh} \leq 12\text{ dB}$). All the subcarriers undergo the same shadowing effect for one user at one instant ([7]). Due to multipath propagation, the received signal on a subcarrier is the sum of several scattered waves. The amplitude of the received signal on each subcarrier has a Rayleigh distribution. The correlation between the signal envelopes of different subcarriers is considered (cf. appendix).

The channel gain $g(u,n)$, of user $u$ on subcarrier $n$ in the serving cell, is summarized as: $g(u,n)=K\ d(u)^{-\alpha}\ a_{sh}(u)\ a_f(u,n)$ where $a_f$ has a Rayleigh distribution and represents the small scale fading. We consider additive white Gaussian noise (AWGN) which is characterized on each subcarrier by a Gaussian random variable $\mathcal{N}(0,\sigma^2)$ with $\sigma^2=N_0W/N$. Let $B$ be the number of interfering cells, the channel gain to interference and noise ratio (CgINR) is $c_g inr(u,n)=g(u,n)/(\sigma^2+I(u,n))$. The level of interference suffered by user $u$ on subcarrier $n$ is expressed as $I(u,n) = \Sigma_{b=1..B} K\ d_b(u)^{-\alpha}\ a_{sh}{}^b(u)\ a_f{}^b(u,n)\ \delta_{b,n}$. In this expression, $d_b(u)$ and $a_{sh}{}^b(u)$ are the distance and the shadowing effect between user $u$ and interfering cell $b$, $a_f{}^b(u,n)$ is the small scale fading on subcarrier $n$; $\delta_{b,n}$ is one if subcarrier $n$ is used in interfering cell $b$, otherwise $\delta_{b,n}$ is zero. In a reuse one deployment with full loading, $\delta_{b,n}=1$ for $1\le b\le B$ and $1\le n\le N$.

### B. System parameters

We consider the downlink of one reference hexagonal cell with one BS and $U$ users. Interferences come from $B$ cells distributed in two rings. Equal power $p$ is allocated to subcarriers ([4]). The signal to interference and noise ratio is $SINR(u,n)=p\ c_g inr(u,n)$. We assume the same MCS for the $N_{sc}=48$ subcarriers of a subchannel. The MCS is determined by the subchannel effective SINR (cf. V) according to Table I ([1]). For simplicity, each user receives one subchannel. Among the $N$ subcarriers (Fast Fourier Transform size), the number of data subcarriers is $N_{data}$. In the scalable version of the physical layer ([2]), the subcarrier spacing $\Delta f$ and the useful symbol duration $T_u=1/\Delta f$ are independent of the bandwidth $W$; $T_u=91.43$ µs. The guard time represents 1/8 of $T_u$: $T_g=11.67$ µs. The total symbol duration is thus $T_s=102.86$ µs.

## III. Subchannelization modes in 802.16

Several modes of subchannelization are described in [1-2] among which can be found FUSC (Full Usage of SubChannels), PUSC (Partial Usage of SubChannels), and AMC (Adaptive modulation and coding). Section III describes these modes in the downlink.

### A. FUSC

#### 1) Subchannel composition

In FUSC (not defined in uplink), subchannels are composed of $N_{sc}$ subcarriers during one OFDM symbol duration. Taking advantage of channel diversity, subchannels are made of subcarriers spread over the frequency band. The bandwidth is divided into $N_{sc}$ groups of $N_{scg}=N_{data}/N_{sc}$ consecutive subcarriers, after excluding the initially assigned pilots. A subchannel is made of one subcarrier from each group. The formula which governs subchannel composition can be summarized as follows: $k_s = GS(s,k) + SS(s,k,DL\_PermBase)$. In this formula, $k_s$ designates the $(k+1)^{th}$ subcarrier of subchannel $s$, $GS$ stands for group selection and $SS$ stands for subcarrier selection.

TABLE I: MODULATIONS AND CODING SCHEMES

| Modulation | Coding Rate | Required SNR (dB) |
|---|---|---|
| QPSK | 1/2 | 6 |
| QPSK | 3/4 | 9 |
| 16-QAM | 1/2 | 12 |
| 16-QAM | 3/4 | 15 |
| 64-QAM | 2/3 | 18 |
| 64-QAM | 3/4 | 21 |

The function $GS$, depends on indexes $s$ and $k$. It indicates the first subcarrier of the group wherein the $(k+1)^{th}$ subcarrier of subchannel $s$ will be picked out (cf. Fig. 1). $GS(s,k)$ is a multiple of $N_{scg}$ where $N_{scg}$ is the number of subcarriers in a group.

$$GS(s,k) = m_{k,s}\ N_{scg}$$
$$m_{k,s} = (k + 13\ s) \bmod N_{sc}$$

Thanks to function $SS$, a specific subcarrier is chosen into the group pointed by $GS(s,k)$. $SS(s,k,DL\_PermBase)$ satisfies: $0\le SS(s,k,DL\_PermBase) \le N_{scg}-1$. The function $SS$ is governed by a permutation list of $N_{scg}$ integers (between 0 and $N_{scg}-1$) which is proper to subchannel $s$ (this list is denoted as $p_s$, see Table II). The parameter $DL\_PermBase$ serves as an offset; it is given by the DL-MAP[1] and differs following the zone[2] of the DL subframe.

$$SS(s,k,IDcell) = \{\ p_s(m_{k,s}\ mod\ N_{scg}) + DL\_PermBase\}\ mod\ N_{scg}$$

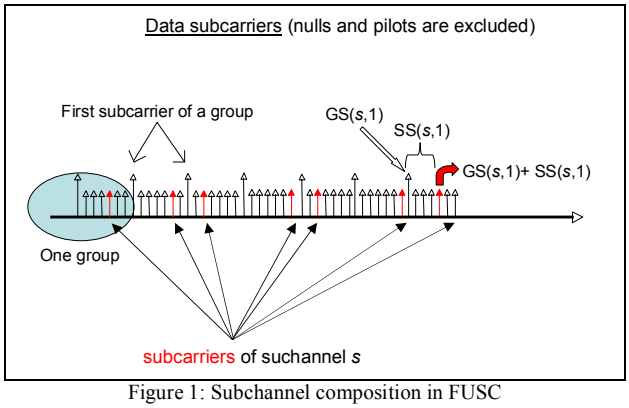


Figure 1: Subchannel composition in FUSC

TABLE II: FUSC PARAMETERS

| | | |
|---|---|---|
| $W$ | Total bandwidth | 10 MHz |
| $N$ | Total number of subcarriers | 1024 |
| $N_{data}$ | Number of data subcarriers | 768 |
| $N_{sc}$ | Number of data subcarriers per subchannel | 48 |
| $N_{scg}$ | Number of data subcarriers per group | 16 |
| $p_0$ | Permutation list: $p_s$ is $p_0$ cyclically shifted to the left $s$ times | [6 14 2 3 10 8 11 15 9 1 13 12 5 7 4 0] |
| $S$ | Number of subchannels | 16 |
| $U$ | Number of users in one cell | 16 |

[1] A broadcast MAC management message.
[2] Contiguous OFDMA symbols using the same subchannelization mode.

*2) Probability of collision*

In this section, two distinct cells are considered. A frequency reuse 1 is assumed, there is no sectorization. When the two cells use the same frequency band, we are interested in evaluating the probability of getting $c$ collisions between subchannels used by each cell.

When a cell uses $L$ subchannels out of $S$, it is called partial loading and the loading factor is $L/S$.

For low values of $L$ (respectively $L$=1 and $L$=2), the FUSC probability density function (PDF) is plotted (resp. Fig.2 and Fig.3) and compared with random subchannelization PDF. In random subchannelization, a subchannel is made of $N_{sc}$ random subcarriers out of $N_{data}$. If both cells use $L$ subchannels, the probability of getting $c$ collisions is:

$$p_{random}(c) = \frac{C_{N_{data}-L\times N_{sc}}^{L\times N_{sc}-c} C_{L\times N_{sc}}^{c}}{C_{N_{data}}^{L\times N_{sc}}}$$

A similar result is developed in [8] for $L$=1. In case of full loading i.e. $L$=$S$, all subcarriers are collided i.e. $p(c) = 0$ if $c < N_{data}$ and $p(c) = 1$ if $c = N_{data}$. It holds for both FUSC and random subchannelization.

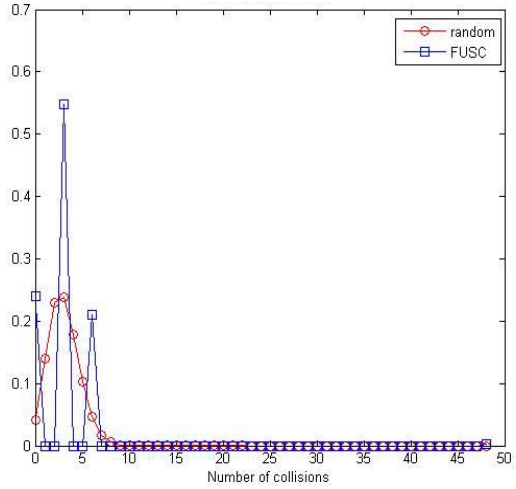


Figure 2: Collision probability density function, loading factor = 1/16

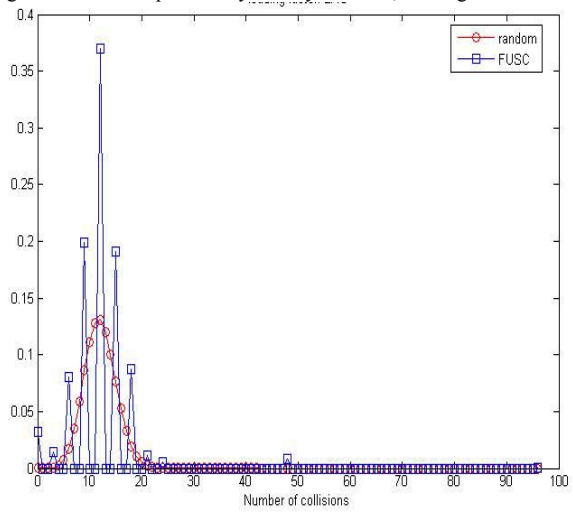


Figure 3: Collision probability density function, loading factor = 2/16

In Fig.2, for $L$=1 in both reference and interfering cells, the FUSC PDF is obtained by exhaustive inspection[3]. In Fig.3, for $L$=2 in both cells, a partial inspection gives a good approximation[4] of the FUSC collision PDF. The FUSC PDF is not "continuous": it is non null for specific values which are not adjacent. For example, in Fig.2, $p(c) = 0$ if $c \notin \{0, 3, 6\}$ and in Fig.3, $p(c) = 0$ if $c \notin \{0, 3, 6, 9, 12, 15, 18, 21, 24, 48, 96\}$. The number of used subcarriers is $L.N_{sc}$ with $N_{sc}$=48. It can thus be seen that FUSC PDF is rather different from random subchannelization PDF. However, the average number of collisions is the same. This gives a simple way to obtain FUSC average number of collisions.

From our simulations[5], we obtained the FUSC average number of collisions versus the loading factor. Based on these figures, a probability of hit for one subcarrier can be derived (cf. Table III). Between two BS with uniform loading, the resulting probability of hit, on one subcarrier, is equal to the loading factor. This result can be found faster knowing that the average number of collisions can be approximated by random subchannelization ($n_{coll} = \sum_c c\ p(c)$).

TABLE III: SUBCARRIER COLLISION PROBALITY AND LOADING FACTOR

| **Simulation input** | Loading factor: $L/S$ | Number of used subcarriers: $n_{used} = L.N_{sc}$ | **Simulation output** | Collision probability for 1 subcarrier: $n_{coll} / n_{used}$ |
|---|---|---|---|---|
| Used subchannels over 16: $L$ | | | Average number of collisions: $n_{coll}$ | |
| 1 | 0.062 | 48 | 3 | 0.062 |
| 2 | 0.125 | 96 | 11.98 | 0.125 |
| 3 | 0.187 | 144 | 26.88 | 0.186 |
| 6 | 0.375 | 288 | 108.17 | 0.375 |
| 10 | 0.625 | 480 | 299.65 | 0.624 |
| 13 | 0.812 | 624 | 504.87 | 0.809 |

## B. PUSC

The (downlink) PUSC mode divides the bandwidth into 6 parts called major groups. It enables another frequency reuse factor than one (in FUSC, only reuse one is possible). By default, segments are composed of 2 consecutive major groups which can be assigned to distinct cells (or distinct sectors of the same cell if sectorization is assumed). Segmentation is possible because subchannels are made of subcarriers over one major group (instead of the whole band in FUSC). Inside one major group, first pilots are assigned; then the remaining subcarriers are partitioned into groups ([1 p.564], ([2 p.530]). A subchannel consists of one subcarrier per group. The formula governing subchannel composition is common to FUSC. Unlike uplink PUSC, pilots are assigned (in each major group) before subchannels composition. It allows thinking that pilots of a major group can be shared by the subchannels of this major group. It is different in uplink PUSC where each subchannel has its own pilots. Regarding probability of collision in PUSC, the PUSC PDF is compared to random

[3] For each $c$, $p(c)$ is averaged over all *DL_PermBase* pairs and all subchannel index pairs.

[4] Exhaustive inspection is long and unnecessary. Here, all subchannel index quadruplets for half *DL_PermBase* pairs are examined.

[5] For each value of $L$, simulation consists in collisions'number averaging over 250 2$L$-tuples of subchannels index for 100 *DL_PermBase* pairs.

subchannelization PDF in [9].

### C. AMC

The main difference of AMC mode is that subcarriers of a subchannel are adjacent instead of being distributed over the bandwidth. The AMC mode allocates 6 bins (defined as 9 adjacent subcarriers including one pilot) to users. Several subchannel types are defined. For instance, the subchannel type $i \times j$ means that $i$ consecutive bins are allocated over $j$ OFDM symbols ([1], cf. Fig.4). In this paper, we are interested in performance of adjacent subcarriers subchannelization (ASS); compared to AMC, the subchannel type is 6×1.

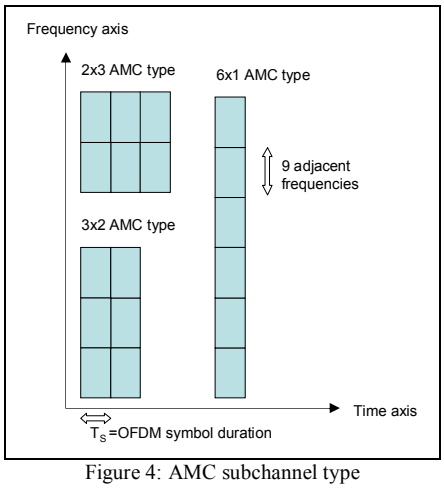


Figure 4: AMC subchannel type

## IV. DYNAMIC SUBCHANNEL COMPOSTION

In this paper, we consider that a subchannel is made of $N_{sc}$ subcarriers over one single OFDM symbol. As sawn in the previous section, subchannels in FUSC mode are predetermined and independent of current CgNR levels of subcarriers. DSA (Dynamic Subcarrier Allocation) algorithms aim at building custom-tailored subchannels. Given the number of subcarriers per user, there are several proposals in the literature to assign specific subcarriers to users in an efficient manner. An optimal algorithm is the Hungarian method ([10]). Among the different heuristics, we describe the proposals of [5] (for its simplicity) and [6] (it exhibits performance close to the Hungarian method). Here, the frequency reuse factor is one, in the downlink the level of interference is known (predictable SINR), so those algorithms can be used.

### A. *Basic Dynamic Assignment* (bDA)

In [5], the users are ordered depending on priorities (1, 2...$U$) arbitrary assigned. Each user chooses its $N_{sc}$ best subcarriers. This is quite unfair for the last users. The authors propose a cyclic order mechanism to change user priorities: at each frame beginning, the priorities are decreased and the first user (priority 1) becomes the last.

### B. *Rate Profit Optimization algorithm* (RPO)

In [6], each receives his best subcarrier if there are no collisions. When users have the same best subcarrier (this is referred to as a conflict), the subcarrier is not blindly given to the best user. In such case, the second best subcarrier of each user is determined. For a competing user, the rate difference between the best and the second best subcarrier is computed. To improve the global rate, the user maximizing this rate difference gets the subcarrier (cf. Fig.5). Further details are given in [6].

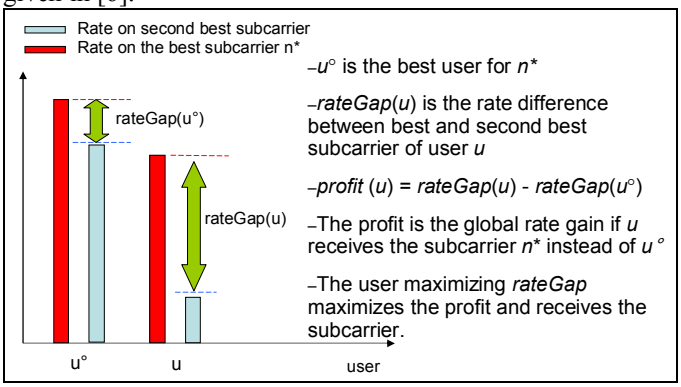


Figure 5: RPO algorithm and profit definition

### C. *Adjacent Subcarrier* (*or contiguous*) *Subchannelization*

Suchannels are composed of $N_{sc}$ adjacent subcarriers one single OFDM symbol (AMC 6×1 subchannel type). If such subchannels are allocated to users regardless of their average channel gain, it is denoted as "random ASS". To improve performance an algorithm may govern subchannel selection for users. A simple algorithm considers users for 1 to $U$; a user receives the available subchannel which exhibits the best average CgINR (this will be referred to as "ASS"). If the number of subcarriers in a coherence bandwidth ($\lfloor B_c / \Delta f \rfloor$) is nearly $N_{sc}$, the different channel gains in a subchannel may be regarded as similar. The signaling overhead is then reduced in ASS compared to individual subcarrier allocation.

## V. SIMULATION RESULTS

Simulation parameters are described in Table IV.

A frequency selective channel is modeled (see Appendix). The coherence bandwidth is often defined as adjacent subcarriers whose correlation coefficient is beyond 0.5 ([11]); the relation between the root mean square (RMS) delay spread is then approximated by: $B_c = 1/2\pi\,\sigma_{rms}$. The channel RMS delay spread of the channel is set as 295ns. The coherence bandwidth is thus 539 kHz. The subchannel size is $N_{sc}\Delta f$ = 524.6 kHz with $N_{sc}$ = 48 and $\Delta f$ =10.93 kHz.

TABLE IV: SIMULATION PARAMETERS

| | |
|---|---|
| Path loss constant: $K$ | $1.4\ 10^{-4}$ |
| Path loss exponent: $\alpha$ | variable |
| Log-normal standard deviation: $\sigma_{sh}$ | 8.9 dB |
| Root mean square delay spread: $\sigma_{RMS}$ | 295 ns |
| Thermal noise: $N_0$ | -174 dBm/Hz |
| Noise Figure at BS receiver | 6 dB |
| Number of data subcarriers: $N_{data}$ | 768 |
| Subcarrier spacing: $\Delta f$ | 10.93 kHz |
| Number of subchannels in one cell: $S$ | 16 |
| Number of users in the reference cell | 16 |
| Number of interfering cells:$B$ | 18 |
| Distance of users in the reference cell | variable |

We focus on one reference cell with one BS and $U$ users. In the reference cell, users are located at the same range of the serving BS, during simulations this common distance varies. The target cell is surrounded by $B$ interfering cells (cf. Fig.6). We consider one sector per cell with omni directional antennas. The reuse factor is one, all frequencies can be used in the interfering cells (the frequency reuse pattern is 1x1x1 according to notations in [9]).

For simplicity, a user receives one subchannel. Subchannel allocation may last several time slots but we only consider snapshots. Spectral efficiency provided by the different algorithms are compared. Results are averaged over 1000 channel state snapshots. The effective SINR of a subchannel $s$ is given by $2^{MIC(s)}$-1 ([10]) where MIC stands for mean instantaneous capacity. The subchannel MIC is the average capacity computed accross $N_{sc}$ subcarriers of the subchannel; the capacity of a subcarrier (allocated to $u$) is expressed as: $c(u,n) = \log_2(1+\text{SINR}(u,n))$.

### A. Global rate

The distance between two BS (denoted as $d_{BS/BS}$) is 2.5 km. The pathloss exponent $\alpha$ is 3.5. The distance of users with their serving BS is around 500 m. Table V gives global rate performance for the different subchannelization schemes. The RPO algorithm exhibits the highest global rate followed by the bDA heuristic. The adjacent subchannelization achieves rather good performance behind bDA. ASS has the advantage to require less signaling overhead than RPO and bDA. Indeed, in ASS, subcarriers within the coherence bandwidth are grouped whereas RPO and bDA require CSI per subcarrier. The FUSC subchannelization and "random ASS" have similar performance. Multi-user diversity gain can not be achieved if CSI is not considered or shows to be outdated (in case of high mobility).

TABLE V: CELL GLOBAL RATE PERFORMANCE

| Subchannelization scheme | RPO | bDA | ASS | Random ASS | FUSC |
|---|---|---|---|---|---|
| GlobalRate (Mbit/s), $d$=500 m | 18.06 | 17.45 | 16.59 | 12.75 | 12.86 |

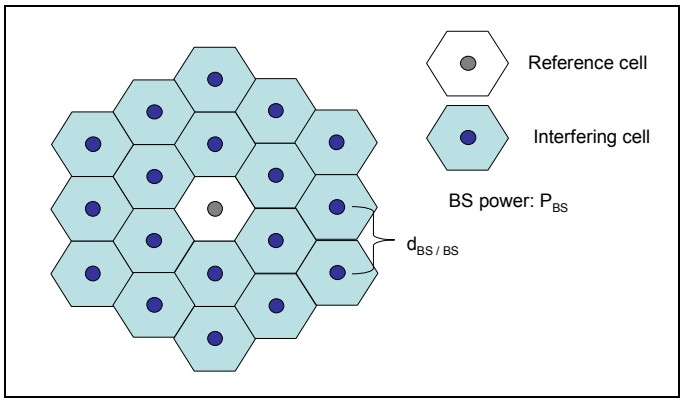


Figure 6: Multi-cell configuration

### B. Influence of propagation model

In Fig.7, the pathloss exponent $\alpha$ varies 2 to 4. The distance between two BS is 2.5 km. As the pathloss exponent $\alpha$ increases, the spectral efficiency increases. High values of $\alpha$ cause severe losses of the useful signal with distance, so that it also decreases the level of interference between the BS. FUSC shows the lowest performance. RPO has the highest spectral efficiency.

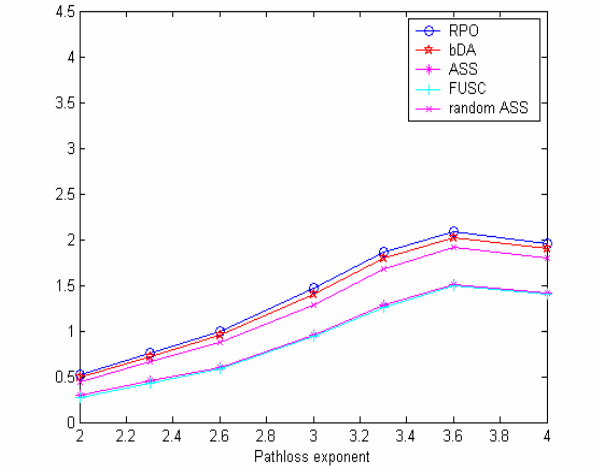


Figure 7: Reuse one, spectral efficiency (bit/s/Hz) vs pathloss exponent

### C. Influence of Inter BS distance

In Fig.8, the distance between two BS varies from 1 to 5 km. The path loss exponent $\alpha$ is 3.5. The performance increases when $d_{BS/BS}$ increases. This is due to the increase of cell isolation. The rate per subchannel is increased by 68% when the $d_{BS/BS}$ is 5 km instead of 2.5 km. In an other hand, the rate per subchannel is decreased by 86% if $d_{BS/BS}$ decreases from 2.5 km to 1 km.

### D. Partial loading

Regarding FUSC subchannelization, partial loading is investigated. In II.A, we expressed the level of interference as $I(u,n) = \Sigma_{b=1..B} K\, d_b(u)^{-\alpha}\, a_{sh}{}^b(u)\, a_f{}^b(u,n)\, \delta_{b,n}$, now $\delta_{b,n}$ is used to simulate partial loading. The probability of collision of one subcarrier is equal to the loading factor $L/S$. So, for a given interfering cell, $\delta_{b,n}$ =1 with probability $L/S$. In this section, $d_{BS/BS}$ =2.5 km; $\alpha$ is 3.5. Users are at the same range of their serving BS, this distance varies in Fig.9 from 0.1 to 1 km. The spectral efficiency decreases with the distance user – serving cell. Indeed, the strength of the useful signal decreases while the level of interference increases. Four loading factors have been considered. The lower the partial loading, the higher the spectral efficiency (for used channels). However, the global rate is low for small loading factors since less subchannels are used (cf. Table VI).

TABLE VI: PARTIAL LOADING AND CELL RATE PERFORMANCE

| FUSC, $d$=500 m | | | | |
|---|---|---|---|---|
| Loading factor | 100% | 80% | 60% | 40% |
| Global rate Mbit/s | 12.35 | 10.46 | 9.25 | 7.49 |
| Rate per subchannel Mbit/s | 0.772 | 0.872 | 1.027 | 1.248 |

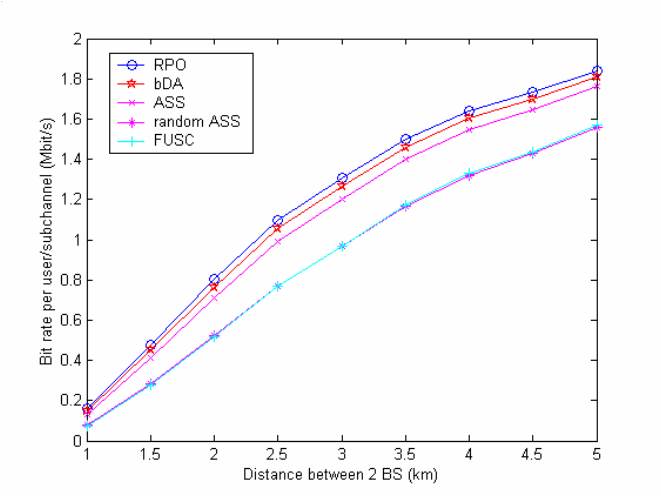


Figure 8: User/subchannel rate versus $d_{BS/BS}$

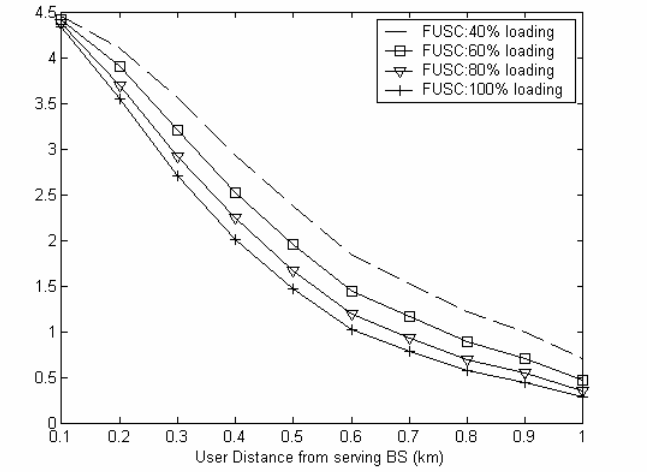


Figure 9: Reuse one, spectral efficiency (bit/s/Hz) vs user distance

## VI. CONCLUSION

In this paper, we have studied different modes of subchannelization for downlink OFDMA. The main modes of IEEE 802.16 have been presented and the performances of FUSC in term of spectral efficiency. A multi-cell context has been considered. Although FUSC exhibits the lowest performance compared to other schemes, FUSC is independent of CSI knowledge so the rate provided is solid guarantee for users. A way to improve FUSC rate guaranty is introduction of partial loading. Spectral efficiency is improved but as fewer subchannels are used, partial loading results in global rate degradation. Individual subcarrier assignment algorithms (Rate Profit Optimization and basic Dynamic Assignment) have been compared with contiguous (or adjacent) subchannelization schemes. The latter performs well with the advantage of requiring less signaling overhead. However, unlike FUSC subchannels, contiguous subchannelization is more sensible to selective fading.

## APPENDIX

Correlation of small scale fading is modeled by a first order Gauss-Markov process. The received signal on a subcarrier is complex ($x$+i$y$). When the number scattered waves is large, $x$ and $y$ are Gaussian by the central limit theorem. The signal envelope $r$ has a Rayleigh distribution; $r=(x^2+y^2)^{1/2}$. Let $\rho_1$, $\rho_2$ and $\rho$ be the correlation coefficients of $x$, $y$ and $r$.

For each subcarrier $n$, $x(n) = \rho_1 x(n\text{-}1)+(1-\rho_1^2)^{1/2}\, w_1(n)$ and $y(n)=\rho_2 y(n\text{-}1)+(1-\rho_2^2)^{1/2}\, w_2(n)$ where $w_1(n)$ (resp. $w_1(n)$) is white Gaussian process independent of $x(n)$ (resp. $y(n)$). Expressions of the correlation coefficient $\rho_1$, $\rho_2$ and $\rho$ can be found in [11]. In Fig.10, it can be seen that the subcarrier correlation decreases with subcarrier spacing. If the coherence bandwidth is defined at $\rho=0.5$, then $B_c=15$ MHz when $\sigma_{rms}=10$ ns whereas $B_c=160$ kHz when $\sigma_{rms}=1\mu$s.

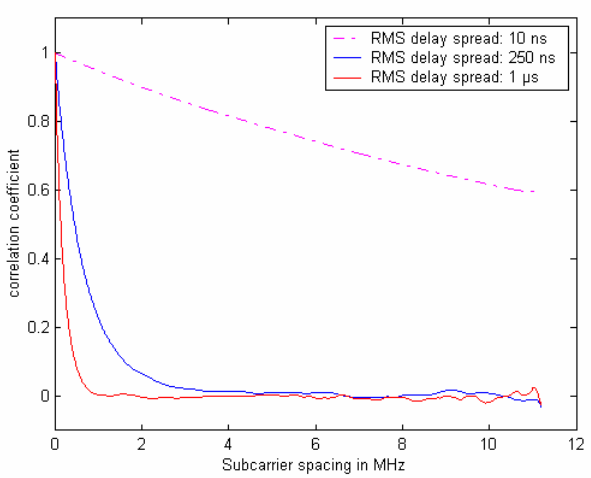


Figure. 10: Correlation coefficient $\rho$ of the signal envelope $r$

## REFERENCES


[1] 802.16-2004. Part 16: Air Interface for Fixed Broadband Wireless Access Systems—IEEE Computer Society and the IEEE Microwave Theory and Techniques Society.

[2] IEEE P802.16e, February 2006. Part 16: Air Interface for Fixed and Mobile Broadband Wireless Access Systems. Amendment2 for Physical and Medium Access Control Layers for Combined Fixed and Mobile Operation in Licensed Bands.

[3] Didem Kivanc, Hui Liu, "Subcarrier Allocation and Power Control for OFDMA", Thirty-Fourth Asilomar Conference on Signals, Systems and Computers, 2000, pp. 147-151 vol.1.

[4] J. Jang, K. B. Lee, "Transmit Power Adaptation for Multiuser OFDM Systems", *IEEE Journal on Communications*, vol. 21, no. 2, pp. 171-178, Feb. 2003.

[5] James Gross, Holger Karl, Frank Fitzek, Adam Wolisz, "Comparison of heuristic and optimal subcarrier assignment algorithms", IEEE International Conference on Wireless Networks 2003, pp. 249-255.

[6] Carle Lengoumbi, Philippe Godlewski, Philippe Martins. « An efficient Subcarrier Assignment Algorithm for Downlink OFDMA ». IEEE 64th Vehicular Technology Conference, Montreal, Canada, 25-28 sept 2006.

[7] C.J. Chang, L. T. H. Lee, Y. S. Chen, "A Utility-Approached Dynamic Radio Resource Allocation Algorithm for Downlink OFDMA Cellular Systems", National Chiao Tung University. VTC Spring 2005.

[8] R. Lerbour, T. Kurt, Y. Le Helloco, B. Breton. « Broadband Wireless Access Interference and capacity Estimation. ». IEEE 64th Vehicular Technology Conference, Montreal, Canada, 25-28 sept 2006.

[9] Wimax Forum, "WIMAX System Evaluation Methodology". Jan 2007.

[10] Christos H Papadimitiou, Kenneth Steigltz. « Combinatorial Optimization, algorithms and complexity ». 1982 Prentice Hall.

[11] M.D. Yacoub, "Foundations of mobile radio engineering". CRC Press Inc. 1993.